Article

Discovery Medicine 2026; 38(212): 2947–2959
https://doi.org/10.24976/Discov.Med.202638212.227

The TOX2/MT1F Axis Mediates Breast Cancer Cell Proliferation and Xenograft Growth

Lei Pan[1], Feixia Ma[1], Yin Duan[1], Xiaoai Lv[1,*]

[1]Department of Breast Surgery, The First Affiliated Hospital of Zhejiang Chinese Medical University (Zhejiang Provincial Hospital of Chinese Medicine), 310006 Hangzhou, Zhejiang, China
*Correspondence: LXA820616@163.com (Xiaoai Lv)
Submitted: 3 July 2026 Revised: 13 August 2026 Accepted: 20 August 2026 Published: 23 September 2026

Background: Aberrant DNA methylation is a key epigenetic mechanism involved in breast cancer (BC) progression. Thymocyte selection-associated high mobility group box 2 (TOX2) has been reported to undergo hypermethylation in BC; however, its functional role and downstream regulatory network remain unclear. This study aimed to explore the biological role of TOX2 and its regulatory interaction with metallothionein-1F (MT1F) in BC progression.

Methods: TOX2 and MT1F expression were modulated in MDA-MB-231 cells using plasmid overexpression and small interfering RNA (siRNA) transfection, and TOX2 and MT1F expression were modulated in MCF-7 cells using plasmid overexpression. Methylation-specific PCR (MSP) and quantitative real-time polymerase chain reaction (qRT-PCR) were performed to assess TOX2 promoter methylation and gene expression levels in BC (MDA-MB-231 and MCF-7) and normal breast cells (MCF-10A). 5-ethynyl-2′-deoxyuridine incorporation and Cell Counting Kit-8 assays were used to calculate the proliferation and viability of MDA-MB-231 and MCF-7 cells. Tumorigenicity *in vivo* was assessed in a nude mouse xenograft model by tumor volume and weight measurements. MT1F expression in both cells and tumor tissues was determined using qRT-PCR.

Results: MDA-MB-231 and MCF-7 cells showed TOX2 promoter methylation and downregulated TOX2 versus MCF-10A cells ($p < 0.001$). TOX2 overexpression markedly inhibited MDA-MB-231 and MCF-7 cell viability and proliferation, accompanied by reduced MT1F expression, whereas TOX2 knockdown exerted opposite effects in MDA-MB-231 cells ($p < 0.001$). In contrast, MT1F overexpression promoted MCF-7 cell proliferation, while its silencing suppressed MDA-MB-231 cell proliferation ($p < 0.01$). Rescue experiments demonstrated that TOX2 and MT1F could reciprocally reverse each other's regulatory effects on BC cell proliferation ($p < 0.05$). *In vivo*, TOX2 knockdown significantly increased xenograft tumor burden, reflected by larger tumor volume and weight, along with elevated MT1F mRNA expression in tumor tissues ($p < 0.001$).

Conclusion: TOX2 downregulation promotes BC cell proliferation and increases xenograft tumor burden, in association with upregulation of MT1F. The TOX2-MT1F-associated regulatory axis may represent a potential therapeutic target in BC. However, further validation in clinical specimens is warranted.

Keywords: TOX2; MT1F; DNA methylation; breast cancer; proliferation

Introduction

With a high incidence rate, breast cancer (BC) is one of the leading malignancies among women globally [1]. Despite decades of research on BC, it remains a dominant cancer-associated cause of disease burden among women [2]. Hence, identifying novel therapeutic targets is necessary for improving BC management.

Given the involvement of epigenetics in carcinogenesis and cancer progression, epigenetic control has been suggested as a potential treatment for BC [3]. DNA methylation, an epigenetic mechanism, regulates gene expression [4] and involves the addition of methyl groups to cytosine at CpG sites [5]. In most cases, hypermethylation silences tumour suppressor expression while hypomethylation promotes oncogene expression [6]. Downregulation of DNA methylation can stimulate gene expression to inhibit BC cell proliferation [7]. Additionally, research has demonstrated that DNA methylation changes hold promise as clinical indicators for BC diagnosis, prognosis, and treatment [8].

Thymocyte selection-associated high mobility group box (TOX), a nuclear DNA-binding factor, regulates transcription by forming multi-protein complexes and changing DNA structure [9]. Dysregulated TOX expression has been reported in several malignancies, including BC, where it may contribute to tumor growth [10]. A previous study has demonstrated that TOX expression is inversely associated with DNA methylation in BC, and higher TOX expression indicates a better prognosis [11]. One member of the TOX family, TOX2, has been proposed as a tumor biomarker that regulates cellular proliferation and death [12]. It remains unmethylated in normal cells while being hypermethylated in BC [13]. Epigenetic inactivation of TOX2 affects multiple pathways by regulating the expression of many genes,

among which metallothionein-1F (MT1F) is significantly upregulated [14].

MTs, cysteine-rich cytosolic proteins, serve as diagnostic and prognostic cancer biomarkers and are implicated in tumourigenesis, tumour growth and metastasis [15]. In BC, overexpression of MT is an unfavourable prognostic characteristic and contributes to increased proliferative capability and reduced apoptotic death of malignant cells [16]. A previous study has indicated a relationship between high MT1 expression and poor prognosis in BC, as higher expression is associated with advanced histologic tumour grade [17]. In Zn^{2+} dyshomeostasis BC cells, an increased level of MT1 isoform, MT1F, has been observed [18]. Moreover, MT1F expression also correlates with histological grade in breast carcinoma [19].

Two critical issues remain unresolved regarding TOX2 and MT1F in BC, despite previous evidence of TOX2 hypermethylation/downregulation and MT1F upregulation: the functional role of TOX2 epigenetic silencing in promoting BC malignancy and whether MT1F serves as a downstream mediator of TOX2's effects. In order to investigate TOX2's function in BC cell proliferation and tumor growth, and to determine whether MT1F is involved in the regulatory effects of TOX2, this study focused on the TOX2/MT1F signaling axis. Our findings may provide a theoretical basis for understanding BC progression and identify potential therapeutic targets for BC.

Materials and Methods

Experimental Animals

Eighteen female BALB/c nude mice (6–7 weeks old, 16–20 g) were obtained from Hangzhou Medical College in China. The animal experiment was approved by the Laboratory Animal Welfare Ethics Committee of Zhejiang Laboratory Animal Center (ZJCLA-IACUC-20020219), in accordance with the ARRIVE Guidelines 2.0.

Cell Culture

Human BC cell lines (MDA-MB-231 (CRM-HTB-26), MCF-7 (HTB-22)), and human breast epithelial cell line MCF-10A (CRL-10317) were obtained from the American Type Culture Collection (Manassas, VA, USA). MDA-MB-231 cells were cultivated at 37 °C without CO_2 using Leibovitz's L-15 Medium (CB007, Epizyme, Shanghai, China) supplemented with 10% fetal bovine serum (FBS, 40131ES76, Yeasen, Shanghai, China). Eagle's Minimum Essential Medium (EMEM, PWL104, MeilunBio, Dalian, China) with 0.01 mg/mL human recombinant insulin (91077C, Merck, Darmstadt, Germany) and 10% FBS was used to cultivate MCF-7 cells (37 °C, 5% CO_2) in an Eppendorf® PROMO incubator (EP2231000761, Merck, Germany). MCF-10A cells were cultured in MEBM with additives from MEGM BulletKit (CC-3150, Lonza Bioscience, Basel, Switzerland) and 100 ng/mL cholera toxin (P7418, Beyotime, Shanghai, China) at 37 °C in 5% CO_2. Every cell line was examined for mycoplasma contamination and verified using short tandem repeat profiling.

Methylation-Specific PCR (MSP)

Cell lysis was achieved with Cell lysis buffer (P0013, Beyotime, China). DNA was further modified by CpGenome Turbo Bisulfite Modification Kit (S7847, Sigma-Aldrich, St. Louis, MO, USA). Subsequently, modified DNA was analyzed using the TaKaRa EpiTaq HS (R110Q, TaKaRa, Beijing, China). PCR was performed using an ABI 7900 thermocycler (4317596, Thermo Fisher Scientific, Waltham, MA, USA) under the following conditions: initial denaturation at 95 °C for 60 s, followed by 40 cycles of incubation at 95 °C for 25 s, 55 °C for 25 s, and 70 °C for 30 s. Electrophoresis was further carried out using the PrimeGel™ Agarose PCR-Sieve (5810A, TaKaRa, Beijing, China). TOX2 (methylated): forward (F) 5′-GTATGTTAAGAGTATTTTTCGGCGT-3′, reverse (R) 5′-TACCCTAAATATTTAAAACGACGCT-3′; TOX2 (unmethylated): 5′-GGTATGTTAAGAGTATTTTTTGGTGT-3′ (F), reverse 5′-TACCCTAAATATTTAAAACAACACT-3′ (R).

Transfection

TOX2 overexpression plasmids (OE-TOX2, RC211560), OE-MT1F (RC205931), overexpression-negative control (OE-NC, PS100001), small interfering RNA targeting TOX2 (si-TOX2, SR313781, 5′-CCAAGAACCCGAAGAAGAAGA-3′ (sense), 5′-UUCUUCUUCGGGUUCUUGGCC-3′ (antisense)), si-MT1F (SR302982, 5′-CCUUUCUCCCAGAUGUAAACA-3′ (sense), 5′-UUUACAUCUGGGAGAAAGGUU-3′ (antisense)) and small interfering RNA negative control (si-NC, 5′-UUCUCCGAACGUGUCACGUTT-3′ (sense), 5′-ACGUGACACGUUCGGAGAATT-3′ (antisense)) were purchased from OriGene Technologies (Wuxi, China). MDA-MB-231 cells were transfected with OE-NC, OE-TOX2, si-NC, si-TOX2, si-MT1F, or si-TOX2 and si-MT1F. Meanwhile, transfection of MCF-7 cells with OE-NC, OE-TOX2, OE-MT1F, or OE-TOX2 and OE-MT1F was performed. MDA-MB-231/MCF-7 cells (2×10^5 cells/well) were cultured in 6-well plates (24 h) to reach 80% confluence. For transfection, the culture medium was replaced with 125 µL serum-free culture medium, and cells were transfected with either with plasmids (2 µg) or siRNA (50 nM), using 4 µL of Lipo8000™ transfection reagent (C0533, Beyotime, China). The transfected complex was incubated with the cells at room temperature (RT) for 6 h, after which the medium was replaced with complete growth medium. Transfected cells were collected at 48 h post-transfection for further analysis. Quantitative real-time polymerase chain reaction (qRT-PCR) was conducted to assess transfection efficiency.

Cell Counting Kit (CCK)-8

A CCK-8 Kit (CA1210, Solarbio, Beijing, China) was utilized to assess cell viability. In 96-well plates, normal and transfected MDA-MB-231/MCF-7 cells (1×10^4 cells/well) were cultured for 24 h and then treated for 4 hwith 10 µL of CCK-8 Reagent. A Synergy Neo2 Hybrid Multimode Reader (450 nm, BioTek, Winooski, VT, USA) was used to measure the absorbance.

5′-ethynyl-2′-deoxyuridine (EdU) Staining

An EdU Staining Proliferation Kit (iFluor 647, ab222421, Abcam, Cambridge, UK) was used to assess cell proliferation. Cells were seeded in 96-well plates at a density of 1×10^4 cells/well and cultured in 200 µL of medium overnight until reaching 70% confluence. Following replacement of 100 µL of culture medium with 2× EdU solution, cells were further incubated (4 h). Cells were permeabilized with 200 µL of 1× Permeabilization Buffer (RT, 30 min), washed twice with 200 µL of Wash Buffer, then incubated in 200 µL of 1× Fixative Solution (RT, 20 min, in the dark). Later, the cells were incubated with 100 µL of Reaction mix (RT, 30 min, in the dark), followed by washing with Wash Buffer and Phosphate-Buffered Saline (PBS, C0221A, Beyotime, China). Cells were stained with 100 µL of 4′,6-diamidino-2-phenylindole (DAPI) Staining Solution (ab228549, Abcam, UK) (RT, 30 min, in the dark). Finally, the stained cells were observed using an Axiolab 5 microscope (ZEISS, Jena, Germany) equipped with a filter for Ex/Em = 649/664 nm (magnification ×200, scale bar = 100 µm). EdU-positive cells (red fluorescence) were quantified using ImageJ software (Version 1.52a, NIH, Bethesda, MD, USA).

Colony Formation Assay

A total of 1000 untreated/transfected cells were seeded in 6-well plates and cultured for 14 days to allow colony formation. After fixation with 200 µL of 4% formaldehyde solution (1004969010, Sigma-Aldrich, St. Louis, MO, USA), viable colonies were stained with 200 µL of 1% crystal violet (V5265, Sigma-Aldrich, St. Louis, MO, USA) (30 min, RT). Cells were photographed using a Nikon D90 camera (Nikon, Tokyo, Japan), and relative colony number was measured using ImageJ software.

Animal Procedure

Short hairpin RNA targeting TOX2 (sh-TOX2, 5′-AGCAAAGAAGGAATATCTGAA-3′) and negative control (sh-NC, 5′-TTCTCCGAGTGTGTCACGT-3′) lentiviral vectors were obtained from Genechem (Shanghai, China). MDA-MB-231 and MCF-7 cells were transduced with sh-TOX2 and sh-NC lentiviral vectors at a multiplicity of infection (MOI) of 10 (viral titer: 1×10^8 TU/mL) for the animal experiments. After 24 h of transduction, the medium was replaced with fresh growth medium.

Every animal was kept in a specific pathogen-free (SPF) environment with a 12-hour light/dark cycle, a controlled temperature of 22 ± 2 °C, a relative humidity of 50–60%, and unlimited access to food and water. 18 BALB/c nude mice were randomly allocated into three groups (9 for MDA-MB-231 cells and 9 for MCF-7 cells): CON, sh-NC, and sh-TOX2. Following trypsinization and PBS washing, MCF-7/MDA-MB-231 cells with sh-TOX2 and sh-NC lentivirus were resuspended in PBS (2×10^6 cells/mL) [20]. For MCF-7 cells, the cell suspension was mixed with Matrigel (#356234, BD Biosciences, San Jose, CA, USA) (1:1) prior to injection; moreover, a 17β-estradiol pellet (0.72 mg, 60-d release) was subcutaneously implanted into the dorsum of each mouse 24 h before cell inoculation. Mice were injected subcutaneously in the left axilla with 100 µL of final cell suspension containing 2×10^5 cells. At 40 days after injection, all mice were anaesthetized with an overdose of 5% isoflurane (1349003, Merck, Darmstadt, Germany) and sacrificed by cervical dislocation. Tumours were extracted from mice, washed in PBS, and the volume and weight was measured [20]. The tumor volume (V) was calculated using the following formula: $V = L \times W^2 \times 0.5$ (L, length; W, width).

Quantitative Real-Time Polymerase Chain Reaction (qRT-PCR)

Cells-/tumours-derived total RNAs (RNAiso Plus; 9108, TaKaRa, China) were reverse-transcribed with PrimeScript™ RT reagent Kit (RR037Q, TaKaRa, China), and RT-PCR was performed using TB Green® Premix Ex Taq™ II (Tli RNaseH Plus, RR820A, TaKaRa, China) on an ABI 7900 thermocycler with the following cycling conditions: 40 cycles of denaturation (95 °C, 15 s), annealing (55 °C, 20 s) and extension (70 °C, 20 s). Data were analyzed by the $2^{-\Delta\Delta CT}$ method [21]. Expressions were normalized to glyceraldehyde-3-phosphate dehydrogenase (GAPDH). TOX2: 5′-TGGCGATGCGGGTTTGAT-3′ (F), 5′-GAGTGGTAGCTGGCTTCGTG-3′ (R); MT1F: 5′-GAAGAGTGAGTGTGAGGCCA-3′ (F), reverse 5′-TGGGAGAAAGGTTGTCCTGG-3′ (R); GAPDH: 5′-AATGGGCAGCCGTTAGGAAA-3′ (F), reverse 5′-GCGCCCAATACGACCAAATC-3′ (R).

Statistical Analysis

GraphPad Prism 8.0 software (GraphPad, CA, USA) was used for statistical analysis, and the data are expressed as mean ± standard deviation (SD). The Shapiro-Wilk test was carried out to assess the normality of the data, and Tukey's post hoc test as well as one-way analysis of variance (ANOVA) were conducted for multi-group comparisons. A $p < 0.05$ was considered statistically significant.

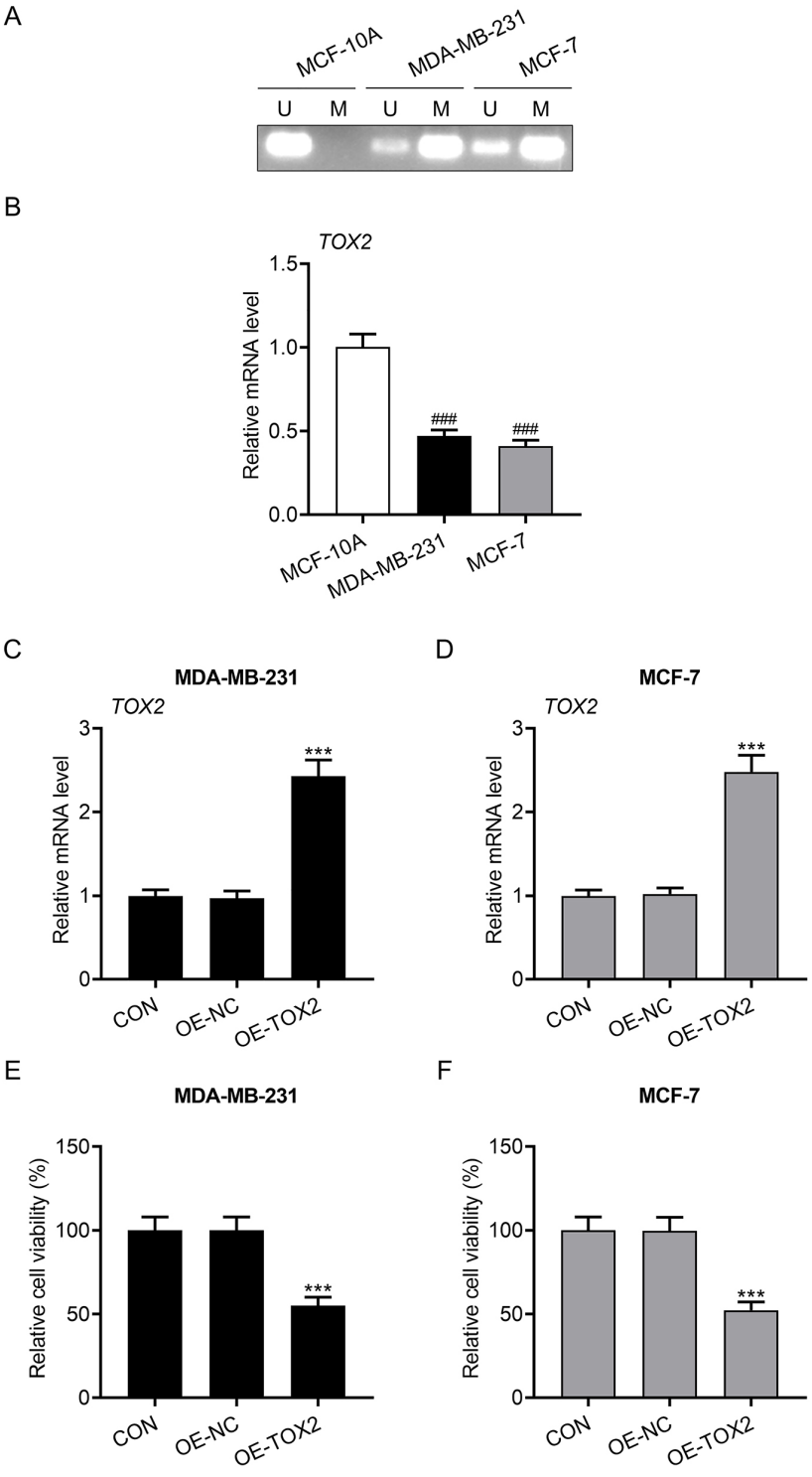

Fig. 1. Thymocyte selection-associated high mobility group box 2 (TOX2) was hypermethylated and lowly expressed in breast cancer (BC) cells, and its overexpression decreased cell viability. (A) TOX2 methylation in MCF-10A/MDA-MB-231/MCF-7 cells (Methylation-specific PCR (MSP)). (B) TOX2 mRNA expression in MCF-10A/MDA-MB-231/MCF-7 cells (Quantitative real-time polymerase chain reaction (qRT-PCR)), with glyceraldehyde-3-phosphate dehydrogenase (GAPDH) as the internal control. (C,D) TOX2 expression in differently treated MDA-MB-231/MCF-7 cells (qRT-PCR), with GAPDH as the internal control. (E,F) Viability in MDA-MB-231/MCF-7 cells (Cell Counting Kit-8 (CCK-8)). CON, normal cells; OE-NC, OE-NC-transfected cells; OE-TOX2, OE-TOX2-transfected cells. Data are expressed as mean ± standard deviation (n = 3 independent biological replicates). $^{\#}$vs. MCF-10A; *vs. OE-NC; $^{\#\#\#}p < 0.001$, $^{***}p < 0.001$.

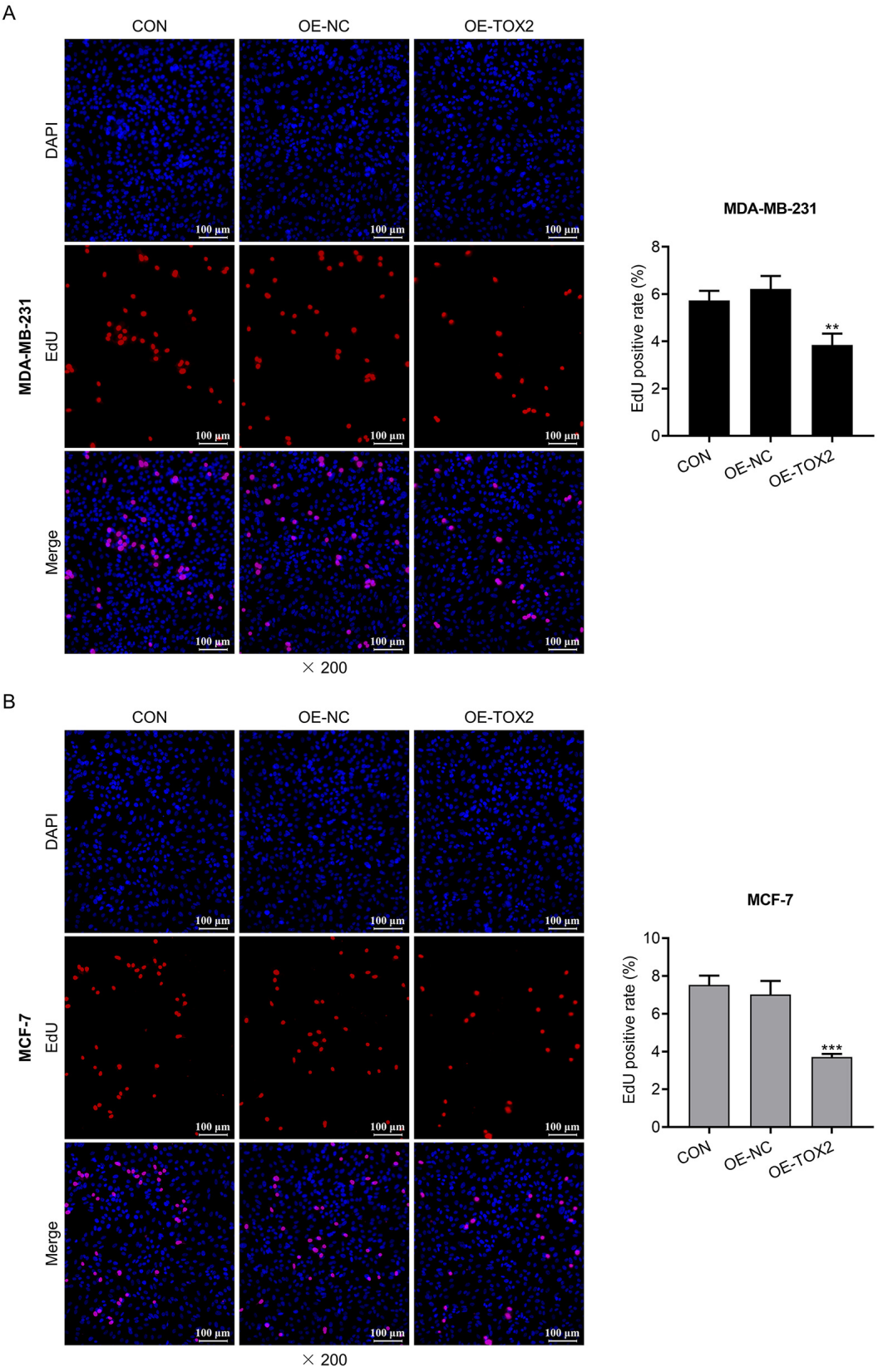

Fig. 2. TOX2 overexpression suppressed MDA-MB-231/MCF-7 cell proliferation. (A,B) MDA-MB-231/MCF-7 cell proliferation (5′-ethynyl-2′-deoxyuridine (EdU) staining) (magnification × 200, scale bar = 100 μm, EdU: red fluorescence). CON, normal cells; OE-NC, OE-NC-transfected cells; OE-TOX2, OE-TOX2-transfected cells. Data are expressed as mean ± standard deviation (n = 3 independent biological replicates). *vs. OE-NC; $^{**}p < 0.01$, $^{***}p < 0.001$.

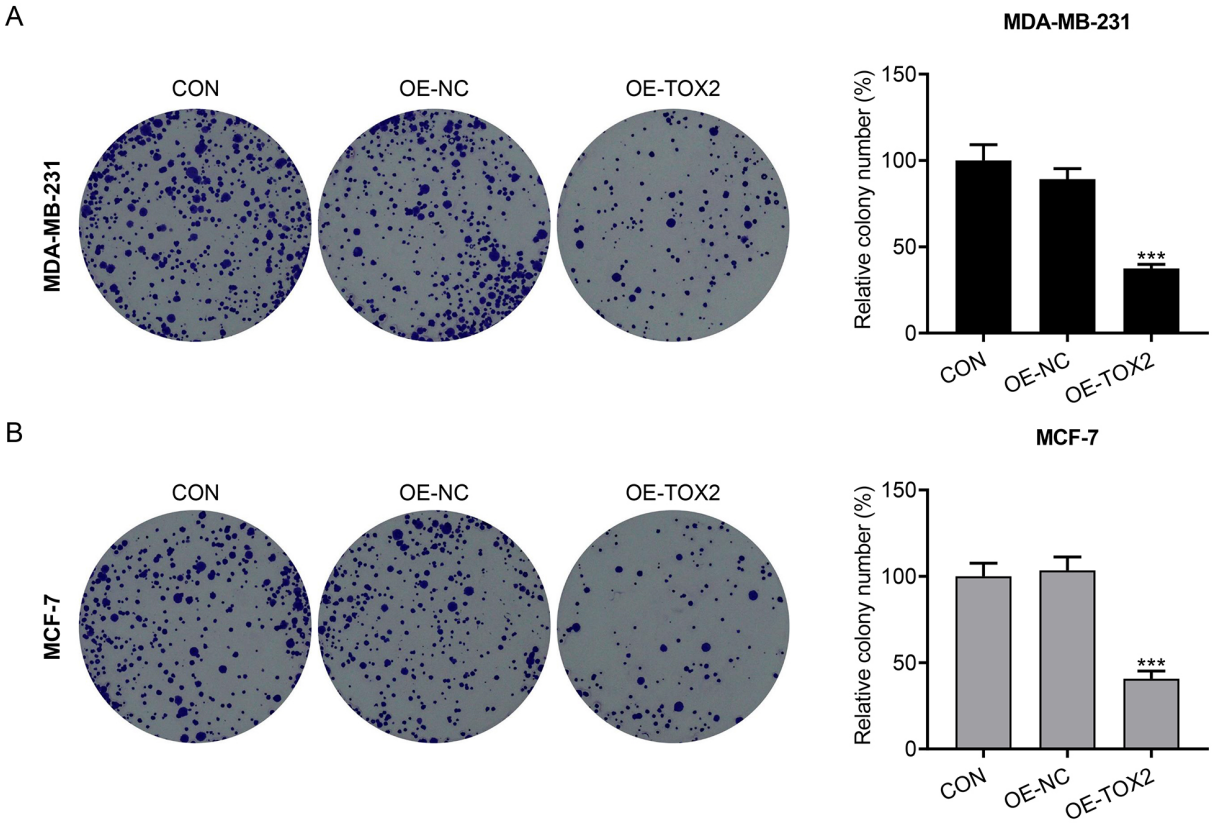

Fig. 3. TOX2 overexpression weakened BC cell colony formation activity. (A,B) Colony numbers in MDA-MB-231/MCF-7 cells (colony formation assay). CON, normal cells; OE-NC, OE-NC-transfected cells; OE-TOX2, OE-TOX2-transfected cells. Data are expressed as mean ± standard deviation (n = 3 biological replicates). *vs. OE-NC; $^{***}p < 0.001$.

Results

TOX2 was Hypermethylated and Downregulated in BC Cells, and Its Overexpression Decreased Cell Viability

MSP assay showed that TOX2 was hypermethylated in MDA-MB-231 and MCF-7 cells relative to MCF-10A cells, in which TOX2 remained unmethylated (Fig. 1A). Consistently, compared with MCF-10A cells, TOX2 expression was significantly lower in MDA-MB-231/MCF-7 cells (Fig. 1B, $p < 0.001$), suggesting a potential association between TOX2 promoter hypermethylation and its transcriptional downregulation. Following OE-TOX2 transfection, TOX2 mRNA was upregulated in MDA-MB-231/MCF-7 cells (Fig. 1C,D, $p < 0.001$), which subsequently induced decreased viability (Fig. 1E,F, $p < 0.001$).

TOX2 Overexpression Suppressed Proliferation

Fewer EdU-positive cells (red fluorescence) were observed in OE-TOX2-transfected cells (Fig. 2A,B, $p < 0.01$) than in OE-NC-transfected cells, suggesting that OE-TOX2 suppressed cell proliferation. The number of colonies was significantly reduced in OE-TOX2-transfected cells compared with OE-NC-transfected cells (Fig. 3A,B, $p < 0.001$).

TOX2 Inversely Regulated MT1F, and the Effects of TOX2 on Cell Viability Were Reversed by MT1F

si-TOX2 transfection reduced TOX2 levels (Fig. 4A, $p < 0.001$) and increased MT1F expression in MDA-MB-231 cells (Fig. 4B, $p < 0.001$), but OE-TOX2 downregulated MT1F in MCF-7 cells (Fig. 4C, $p < 0.001$). MT1F was upregulated in OE-MT1F-transfected MCF-7 cells, yet significantly downregulated in si-MT1F-transfected MDA-MB-231 cells (Fig. 4D,E, $p < 0.001$). si-TOX2 promoted MDA-MB-231 cell viability (Fig. 4F, $p < 0.001$) while si-MT1F exhibited opposite effects (Fig. 4F, $p < 0.001$). Moreover, co-transfection experiments showed that si-TOX2 and si-MT1F partially rescued each other's effects on MDA-MB-231 cell viability (Fig. 4F, $p < 0.01$). OE-TOX2 reduced the viability of MCF-7 cells (Fig. 4G, $p < 0.001$), whereas OE-MT1F exerted the opposite effect (Fig. 4G, $p < 0.001$). In addition, OE-TOX2 (Fig. 4G, $p < 0.001$) and OE-MT1F (Fig. 4G, $p < 0.001$) reversed each other's effects on MCF-7 cell viability.

Effects of TOX2 on MDA-MB-231/MCF-7 Cell Proliferation Were Reversed by MT1F

EdU-positive cells (red) were significantly more abundant in the si-TOX2 group than in the si-NC group (Fig.

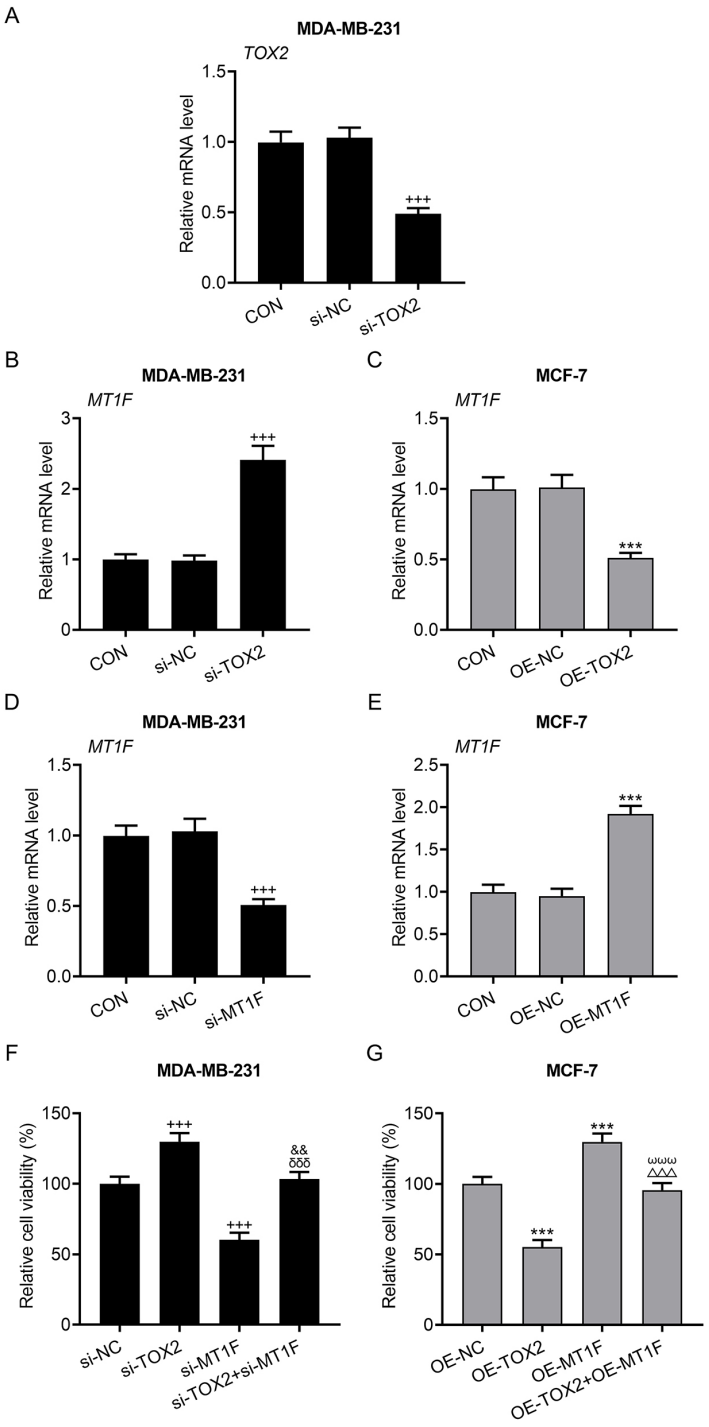

Fig. 4. TOX2 inversely regulated MT1F, and the effects of TOX2 on BC cell viability were reversed by MT1F. (A) TOX2 mRNA expression in MDA-MB-231 cells (qRT-PCR), with GAPDH as the loading control. (B–E) MT1F mRNA expression in MDA-MB-231/MCF-7 cells (qRT-PCR), with GAPDH as an endogenous control. (F,G) MDA-MB-231/MCF-7 cell viability (CCK-8 assay). CON, normal cells; si-NC, si-NC-transfected MDA-MB-231 cells; si-TOX2, si-TOX2-transfected MDA-MB-231 cells; si-MT1F, si-MT1F-transfected MDA-MB-231 cells; si-TOX2+si-MT1F, MDA-MB-231 cells co-transfected with si-TOX2 and si-MT1F; OE-NC, OE-NC-transfected MCF-7 cells; OE-TOX2, OE-TOX2-transfected MCF-7 cells; OE-MT1F, OE-MT1F-transfected MCF-7 cells; OE-TOX2+OE-MT1F, MCF-7 cells co-transfected with OE-TOX2 and OE-MT1F. Data are expressed as mean ± standard deviation (n = 3 independent biological replicates). $^{+}$vs. si-NC; *vs. OE-NC; $^{\&}$vs. si-TOX2; $^{\delta}$vs. si-MT1F; $^{\omega}$vs. OE-TOX2; $^{\triangle}$vs. OE-MT1F; $^{+++}p < 0.001$, $^{***}p < 0.001$, $^{\&\&}p < 0.01$, $^{\delta\delta\delta}p < 0.001$, $^{\omega\omega\omega}p < 0.001$, $^{\triangle\triangle\triangle}p < 0.001$.

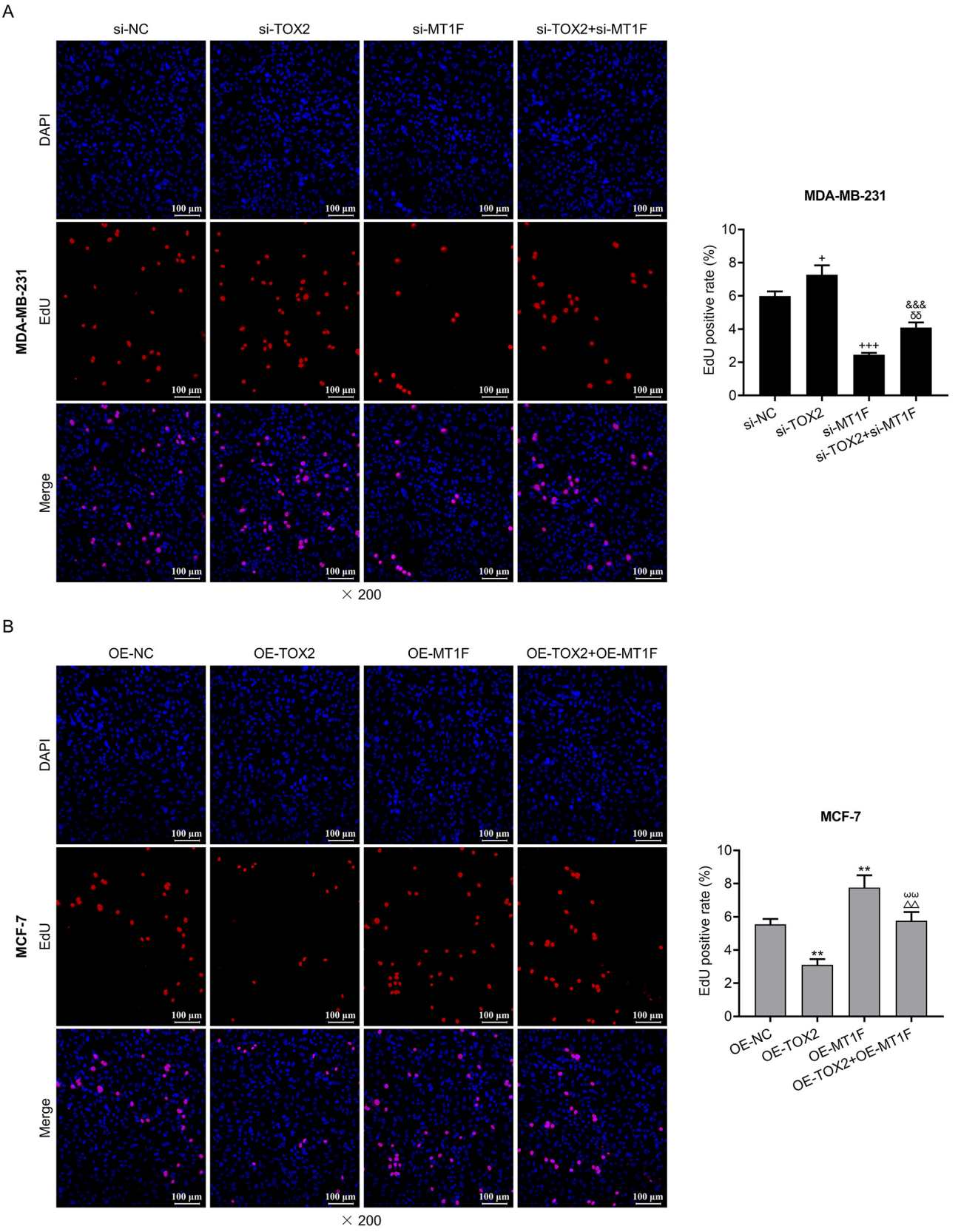

Fig. 5. The roles of TOX2 in BC cell proliferation were reversed by MT1F. (A,B) MDA-MB-231/MCF-7 cell proliferation (EdU staining) (magnification ×200, scale bar = 100 μm, EdU: red fluorescence). Data are expressed as mean ± standard deviation (n = 3 independent biological replicates). $^{+}$vs. si-NC; *vs. OE-NC; $^{\&}$vs. si-TOX2; $^{\delta}$vs. si-MT1F; $^{\omega}$vs. OE-TOX2; $^{\triangle}$vs. OE-MT1F; $^{+}p < 0.05$, $^{+++}p < 0.001$, $^{**}p < 0.01$, $^{\&\&\&}p < 0.001$, $^{\delta\delta}p < 0.01$, $^{\omega\omega}p < 0.01$, $^{\triangle\triangle}p < 0.01$.

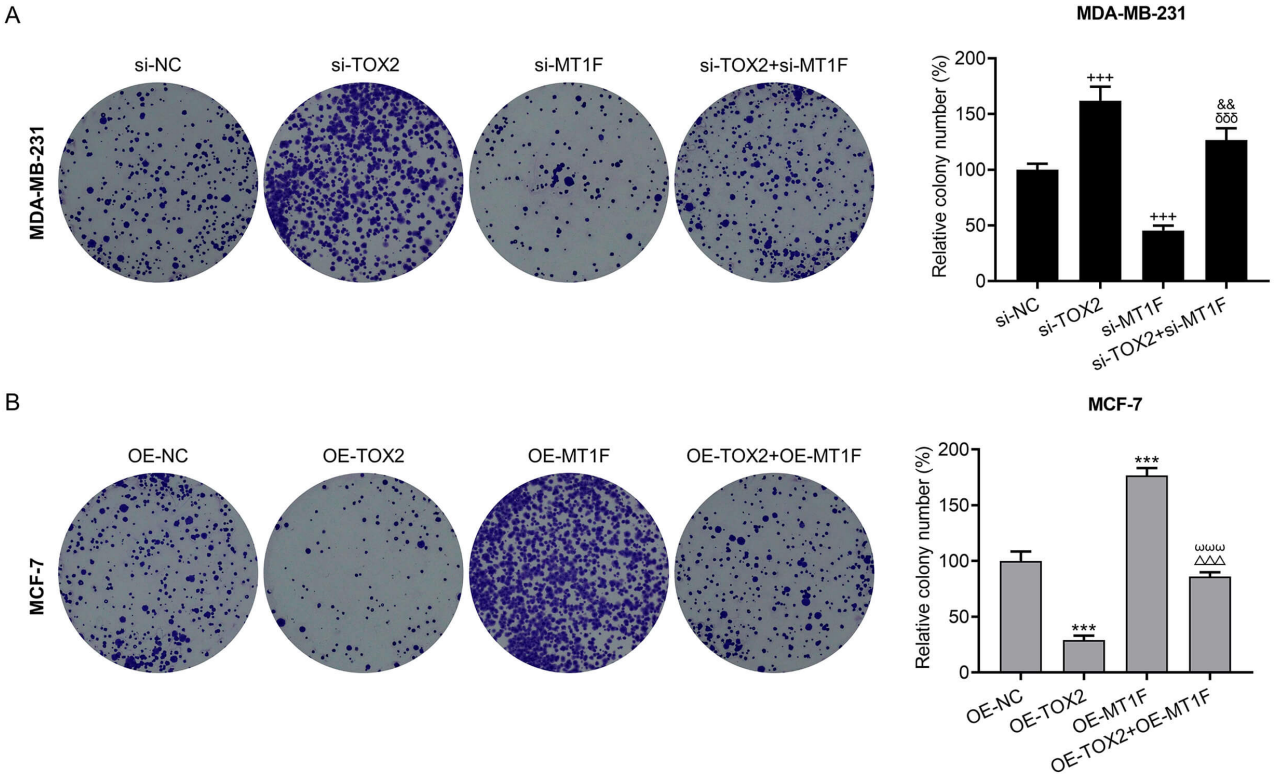

Fig. 6. Effects of TOX2 on colony formation in BC cells were offset by MT1F. (A,B) Colony formation capabilities of MDA-MB-231 and MCF-7 cells (colony formation assay). Data are expressed as mean ± standard deviation (n = 3 biological replicates). $^{+}$vs. si-NC; *vs. OE-NC; $^{\&}$vs. si-TOX2; $^{\delta}$vs. si-MT1F; $^{\omega}$vs. OE-TOX2; $^{\Delta}$vs. OE-MT1F; $^{+++}p < 0.001$, $^{***}p < 0.001$, $^{\&\&}p < 0.01$, $^{\delta\delta\delta}p < 0.001$, $^{\omega\omega\omega}p < 0.001$, $^{\Delta\Delta\Delta}p < 0.001$.

5A, $p < 0.05$), whereas the si-MT1F group exhibited significantly fewer EdU-positive cells (Fig. 5A, $p < 0.001$). MT1F depletion attenuated the si-TOX2-induced enhancement of MDA-MB-231 cell proliferation, whereas TOX2 knockdown abolished the inhibitory effect of si-MT1F on MDA-MB-231 cell proliferation (Fig. 5A, $p < 0.01$). OE-TOX2 inhibited MCF-7 cell proliferation (red fluorescence), whereas OE-MT1F exerted the opposite effect (Fig. 5B, $p < 0.01$). Moreover, OE-TOX2 and OE-MT1F partially reversed each other's effects on MCF-7 cell proliferation (red fluorescence, Fig. 5B, $p < 0.01$).

Effects of TOX2 on Colony Formation Were Offset by MT1F

The ability to form colonies of MDA-MB-231 cells was improved by TOX2 knockdown (Fig. 6A, $p < 0.001$), whereas knockdown of MT1F exerted the opposite effect (Fig. 6A, $p < 0.001$). In addition, si-TOX2 reversed si-MT1F-induced suppression of MDA-MB-231 cell proliferation (Fig. 6A, $p < 0.001$), while si-MT1F weakened the stimulating activity of si-TOX2 on MDA-MB-231 cell proliferation (Fig. 6A, $p < 0.01$). Relative colony number was reduced in MCF-7 cells after transfection with OE-TOX2 (Fig. 6B, $p < 0.001$), an effect that was abolished by OE-MT1F (Fig. 6B, $p < 0.001$). OE-MT1F augmented the colony formation capacity of MCF-7 cells (Fig. 6B, $p < 0.001$), whereas this effect was attenuated by OE-TOX2 (Fig. 6B, $p < 0.001$).

TOX2 Knockdown Increased Final Tumor Burden and MT1F Expression in Tumour Tissues

Fig. 7A,B shows that TOX2 expression in the sh-TOX2 group was substantially lower than that in the sh-NC group ($p < 0.001$). In nude mice treated with MDA-MB-231 cells or MCF-7 cells, knockdown of TOX2 significantly increased the final tumor volume and weight ($p < 0.001$) (Fig. 7C,D, $p < 0.001$) at the endpoint of the experiment. MT1F was elevated in tumor tissues with suppression of TOX2 (Fig. 7E,F, $p < 0.001$).

Discussion

Aberrant DNA hypermethylation may serve as a potential biomarker for the diagnosis of BC [22]. This study showed that hypermethylation of TOX2 promoted the growth of BC cells by regulating MT1F.

Hypermethylation of the TOX2 promoter has been found in many cancers [14]. In BC, TOX2 is differentially methylated, and higher TOX2 methylation appears in high-risk patients [23]. In BC, TOX2 expression is negatively

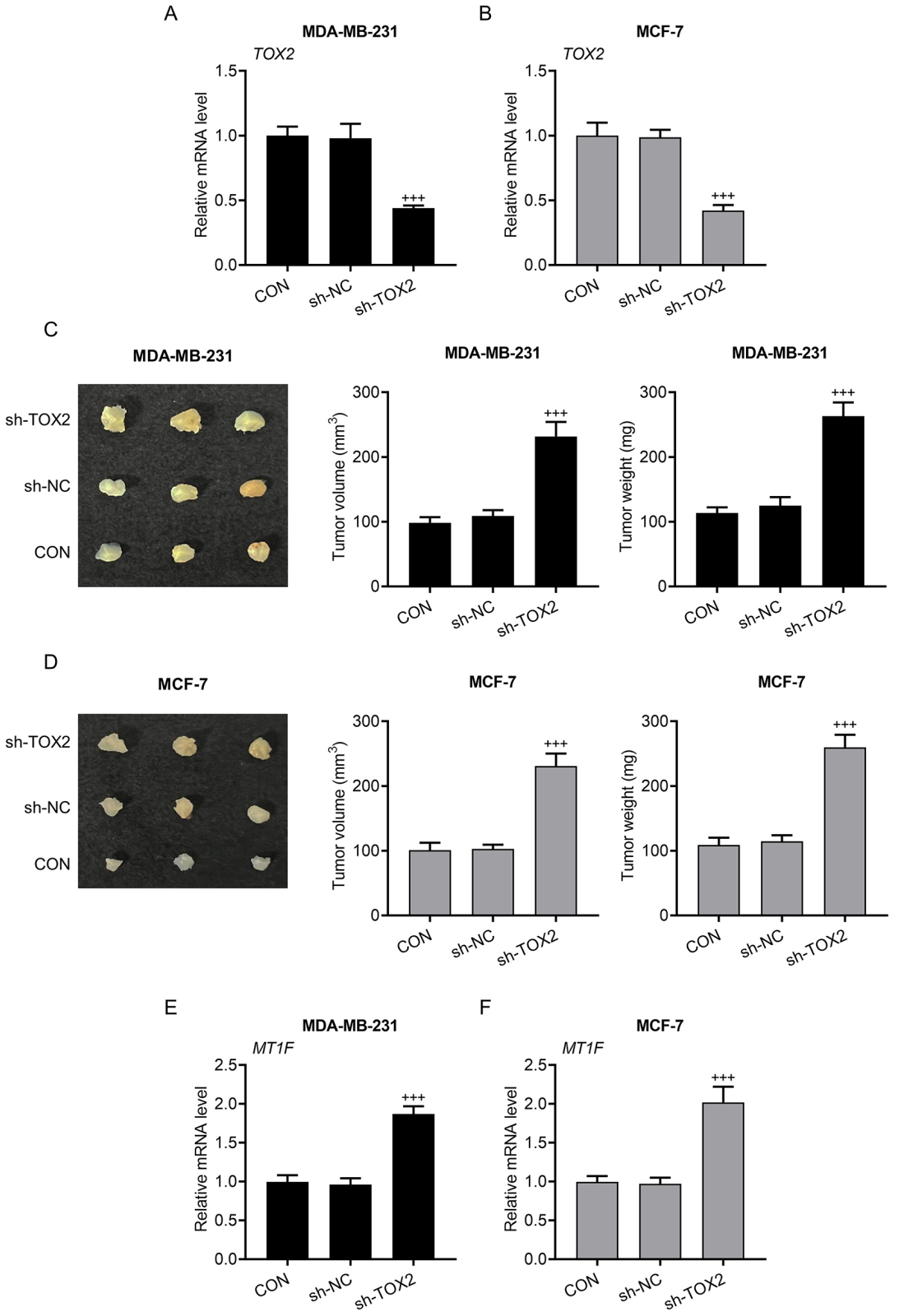

Fig. 7. TOX2 knockdown in BC cells facilitated nude mice tumour bearing and MT1F expression in tumour tissues. (A,B) TOX2 mRNA expression in tumour tissues (qRT-PCR), with GAPDH as an endogenous control. (C,D) Volume and weight of subcutaneous tumours extracted from differently treated nude mice. (E,F) MT1F expression in tumour tissues (qRT-PCR), with GAPDH as an internal reference. All experiments were performed in triplicate (3 mice/group). $^{+}$vs. sh-NC; $^{+++}p < 0.001$.

associated with tumor purity [11]. Similarly, in the current study, TOX2 was unmethylated in normal breast cells but hypermethylated in cancer cell lines. Moreover, TOX2 expression was low in BC cells. This association suggests a potential link between TOX2 promoter hypermethylation and its transcriptional downregulation, although a direct causal relationship requires further experimental validation through demethylation intervention. It is well known that during tumour progression, DNA methylation contributes to the silencing of tumor suppressor genes [24]. This is consistent with a previous study that demonstrated lower TOX2 levels in BC owing to TOX2 hypermethylation [14].

Natural killer (NK) cells are capable of mediating anti-tumour responses by inducing cellular apoptosis [25]. Accumulating evidence has identified TOX2 as an important regulator of NK cell development and function, with TOX2 overexpression promoting NK cell maturation [12]. In addition, targeted inhibition of TOX2 has been reported to suppress the proliferation of lymphocytic malignancies while restoring T-cell-mediated antitumor immunity [26]. However, TOX2 can dampen colorectal cancer by inhibiting mTOR signaling [27]. These studies revealed that its activity is context-dependent. Consistent with these findings, our study demonstrated that TOX2 overexpression significantly suppressed BC cell viability, proliferation, and colony formation, whereas TOX2 silencing exerted the opposite effects. Collectively, TOX2 inhibits tumorigenesis, and its downregulation may promote BC progression.

MT1F is downregulated in gastric cancer and is a potential diagnostic/prognostic marker associated with favorable prognosis [28]. High MT1F expression has been reported to indicate short overall survival and disease-specific survival of patients with low-grade glioma. Upregulated MT1F expression has been observed in BC cells exposed to $CdCl_2$, indicating its role as a tumour promoter [29]. Previous research has demonstrated that MT is associated with increased proliferative capacity in BC cells [30]. Nevertheless, the molecular mechanisms underlying the functions of MT1F in BC cells remain unknown. This study revealed that MT1F overexpression exerted oncogenic effects in BC by maintaining cancer cell viability and stimulating cell growth, whereas MT1F knockdown exerted tumour-suppressive effects in BC cells. Furthermore, we found that TOX2 could downregulate MT1F, and MT1F knockdown reversed the pro-proliferative effect of TOX2 silencing in BC cells. In addition, an *in vivo* assay demonstrated that TOX2 deletion also facilitated final tumor burde and elevated MT1F expression. Together, these findings indicate that MT1F contributes to the oncogenic pathways driven byTOX2 silencing in BC.

Several limitations should be noted in this work. First, the sample size of our *in-vivo* experiments is relatively small, which may affect the robustness of the statistical results. In the future, a larger sample size will be needed for more in-depth research. Second, the results were primarily derived from cell and animal investigations and were not validated in large clinical cohorts or primary BC patient tissues; thus, the clinical significance and translational potential of our findings require further verification. Third, we only detected TOX2 promoter methylation via MSP assay, whereas demethylation intervention experiments such as 5-Aza treatment were not performed to establish a causal link between TOX2 hypermethylation and its reduced expression. Fourth, the downstream signaling cascades regulated by MT1F were not explored in the present study. Fifth, our mechanistic conclusions were predominantly derived from mRNA expression data, as TOX2 or MT1F protein levels were not examined in BC cells or xenograft tumor tissues; therefore, the functional regulation at the translational level and the reliability of the proposed TOX2–MT1F association remain unverified. Future studies should address these limitations more thoroughly.

Conclusion

In conclusion, this study revealed that TOX2 downregulation promotes BC cell proliferation and increases xenograft tumor burden, in association with upregulation of MT1F. Furthermore, the study provides the first evidence of the TOX2-MT1F signaling axis in BC, providing novel insights into molecular mechanisms underlying BC progression. These findings suggest a potential therapeutic avenue, although further validation in clinical specimens and patient cohorts is required before translational application.

Availability of Data and Materials

The datasets used or analyzed during the current study are available from the corresponding author upon reasonable request.

Author Contributions

LP and FXM designed the research study; LP, FXM, YD and XAL performed the research; YD and XAL collected and analyzed the data. LP and FXM have been involved in drafting the manuscript and all authors have been involved in revising it critically for important intellectual content. All authors gave final approval of the version to be published. All authors have participated sufficiently in the work to take public responsibility for appropriate portions of the content and agreed to be accountable for all aspects of the work in ensuring that questions related to its accuracy or integrity.

Ethics Approval and Consent to Participate

The animal experiment was performed with the approval of the Laboratory Animal Welfare Ethics Committee of Zhejiang Laboratory Animal Center (ZJCLA-IACUC-20020219) in accordance with the ARRIVE Guidelines 2.0.

Acknowledgment

Not applicable.

Funding

This work was supported by the General Project of Education Department of Zhejiang Province [grant number: Y202351370] and the Zhejiang Provincial Medical and Health Science and Technology Program under Health Commission of Zhejiang Province [grant number: 2024KY1203].

Conflict of Interest

The authors declare no conflict of interest.

References

[1] Cai Y, Dai F, Ye Y, Qian J. The global burden of breast cancer among women of reproductive age: a comprehensive analysis. Scientific Reports. 2025; 15: 9347. https://doi.org/10.1038/s41598-025-93883-9

[2] GBD 2023 Breast Cancer Collaborators. Global, regional, and national burden of breast cancer among females, 1990-2023, with forecasts to 2050: a systematic analysis for the Global Burden of Disease Study 2023. The Lancet. Oncology. 2026; 27: 302–326. https://doi.org/10.1016/S1470-2045(25)00730-2

[3] Maqsood Q, Khan MU, Fatima T, Khalid S, Malik ZI. Recent Insights Into Breast Cancer: Molecular Pathways, Epigenetic Regulation, and Emerging Targeted Therapies. Breast Cancer : Basic and Clinical Research. 2025; 19: 11782234251355663. https://doi.org/10.1177/11782234251355663

[4] Seem K, Kaur S, Kumar S, Mohapatra T. Epigenome editing for targeted DNA (de)methylation: a new perspective in modulating gene expression. Critical Reviews in Biochemistry and Molecular Biology. 2024; 59: 69–98. https://doi.org/10.1080/10409238.2024.2320659

[5] Bhootra S, Jill N, Shanmugam G, Rakshit S, Sarkar K. DNA methylation and cancer: transcriptional regulation, prognostic, and therapeutic perspective. Medical Oncology (Northwood, London, England). 2023; 40: 71. https://doi.org/10.1007/s12032-022-01943-1

[6] Agarwal N, Jha AK. DNA hypermethylation of tumor suppressor genes among oral squamous cell carcinoma patients: a prominent diagnostic biomarker. Molecular Biology Reports. 2024; 52: 44. https://doi.org/10.1007/s11033-024-10144-0

[7] Gong W, Fang P, Leng M, Shi Y. Promoting GSDME expression through DNA demethylation to increase chemosensitivity of breast cancer MCF-7 / Taxol cells. PloS One. 2023; 18: e0282244. https://doi.org/10.1371/journal.pone.0282244

[8] Williams S, Clark SJ, Pidsley R, Stirzaker C. DNA methylation biomarkers for the diagnosis and treatment management of breast cancer: where are we now? Epigenomics. 2025; 17: 1107–1122. https://doi.org/10.1080/17501911.2025.2548755

[9] Maestre L, García-García JF, Jiménez S, Reyes-García AI, García-González Á, Montes-Moreno S, et al. High-mobility group box (TOX) antibody a useful tool for the identification of B and T cell subpopulations. PloS One. 2020; 15: e0229743. https://doi.org/10.1371/journal.pone.0229743

[10] Chen T, Li Q, Zhang X, Long R, Wu Y, Wu J, et al. TOX expression decreases with progression of colorectal cancers and is associated with CD4 T-cell density and Fusobacterium nucleatum infection. Human Pathology. 2018; 79: 93–101. https://doi.org/10.1016/j.humpath.2018.05.008

[11] Arora M, Kumari S, Singh J, Chopra A, Chauhan SS. Expression pattern, regulation, and clinical significance of TOX in breast cancer. Cancer Immunology, Immunotherapy : CII. 2021; 70: 349–363. https://doi.org/10.1007/s00262-020-02689-3

[12] Zhou J, Toh SHM, Tan TK, Balan K, Lim JQ, Tan TZ, et al. Super-enhancer-driven TOX2 mediates oncogenesis in Natural Killer/T Cell Lymphoma. Molecular Cancer. 2023; 22: 69. https://doi.org/10.1186/s12943-023-01767-1

[13] Zeng D, Lin H, Cui J, Liang W. TOX3 is a favorable prognostic indicator and potential immunomodulatory factor in lung adenocarcinoma. Oncology Letters. 2019; 18: 4144–4152. https://doi.org/10.3892/ol.2019.10748

[14] Tessema M, Yingling CM, Grimes MJ, Thomas CL, Liu Y, Leng S, et al. Differential epigenetic regulation of TOX subfamily high mobility group box genes in lung and breast cancers. PloS One. 2012; 7: e34850. https://doi.org/10.1371/journal.pone.0034850

[15] Xing Y, Li G, Li G, Xu J, Zhang T, Li M, et al. MT1H inhibits the growth of gastric cancer by regulating SLC6A19/TTC39B/ADM2 and activating p53-dependent autophagy. Scientific Reports. 2025; 15: 9339. https://doi.org/10.1038/s41598-025-91319-y

[16] Kepinska M, Kizek R, Milnerowicz H. Metallothionein and Superoxide Dismutase-Antioxidative Protein Status in Fullerene-Doxorubicin Delivery to MCF-7 Human Breast Cancer Cells. International Journal of Molecular Sciences. 2018; 19: 3253. https://doi.org/10.3390/ijms19103253

[17] Shahmoradipour P, Emamzadeh R. Advances in the use of MT1-MMP-targeted nanobodies and peptides for therapeutic delivery in triple-negative breast cancer. Biomedicine & Pharmacotherapy = Biomedecine & Pharmacotherapie. 2026; 194: 118944. https://doi.org/10.1016/j.biopha.2025.118944

[18] Barman SK, Zaman MS, Veljanoski F, Malladi CS, Mahns DA, Wu MJ. Expression profiles of the genes associated with zinc homeostasis in normal and cancerous breast and prostate cells. Metallomics : Integrated Biometal Science. 2022; 14: mfac038. https://doi.org/10.1093/mtomcs/mfac038

[19] Calaf GM, Crispin LA, Roy D, Aguayo F, Muñoz JP, Bleak TC. Gene Signatures Induced by Ionizing Radiation as Prognostic Tools in an In Vitro Experimental Breast Cancer Model. Cancers. 2021; 13: 4571. https://doi.org/10.3390/cancers13184571

[20] Fan Y, Wang X, Li Y. IFI30 expression predicts patient prognosis in breast cancer and dictates breast cancer cells proliferation via regulating autophagy. International Journal of Medical Sciences. 2021; 18: 3342–3352. https://doi.org/10.7150/ijms.62870

[21] Chen Z, Halford NG, Liu C. Real-Time Quantitative PCR: Primer Design, Reference Gene Selection, Calculations and Statistics. Metabolites. 2023; 13: 806. https://doi.org/10.3390/metabo13070806

[22] Chen Z, Jiang H, Qin Q, Li Q, Hong L. DNA methylation signatures provide novel diagnostic biomarkers and predict responses of immune therapy for breast cancer. Frontiers in Genetics. 2024; 15: 1403907. https://doi.org/10.3389/fgene.2024.1403907

[23] Crujeiras AB, Diaz-Lagares A, Stefansson OA, Macias-Gonzalez M, Sandoval J, Cueva J, et al. Obesity and menopause modify the epigenomic profile of breast cancer. Endocrine-related Cancer. 2017; 24: 351–363. https://doi.org/10.1530/ERC-16-0565

[24] Nishiyama A, Nakanishi M. Navigating the DNA methylation landscape of cancer. Trends in Genetics : TIG. 2021; 37: 1012–1027. https://doi.org/10.1016/j.tig.2021.05.002

[25] Portale F, Di Mitri D. NK Cells in Cancer: Mechanisms of Dysfunction and Therapeutic Potential. International Journal of

Molecular Sciences. 2023; 24: 9521. https://doi.org/10.3390/ijms24119521

[26] Liang C, Huang S, Zhao Y, Chen S, Li Y. TOX as a potential target for immunotherapy in lymphocytic malignancies. Biomarker Research. 2021; 9: 20. https://doi.org/10.1186/s40364-021-00275-y

[27] Yang M, Huang Q, Li C, Jiang Z, Sun J, Wang Z, et al. TOX Acts as a Tumor Suppressor by Inhibiting mTOR Signaling in Colorectal Cancer. Frontiers in Immunology. 2021; 12: 647540. https://doi.org/10.3389/fimmu.2021.647540

[28] He J, Jiang X, Yu M, Wang P, Fu L, Zhang G, et al. MTF1 has the potential as a diagnostic and prognostic marker for gastric cancer and is associated with good prognosis. Clinical & Translational Oncology : Official Publication of the Federation of Spanish Oncology Societies and of the National Cancer Institute of Mexico. 2023; 25: 3241–3251. https://doi.org/10.1007/s12094-023-03198-2

[29] Luparello C. Cadmium-Associated Molecular Signatures in Cancer Cell Models. Cancers. 2021; 13: 2823. https://doi.org/10.3390/cancers13112823

[30] Zaman MS, Barman SK, Corley SM, Wilkins MR, Malladi CS, Wu MJ. Transcriptomic insights into the zinc homeostasis of MCF-7 breast cancer cells via next-generation RNA sequencing. Metallomics : Integrated Biometal Science. 2021; 13: mfab026. https://doi.org/10.1093/mtomcs/mfab026